ELSEVIER

Biochimica et Biophysica Acta 1463 (2000) 131–141

BIOCHIMICA ET BIOPHYSICA ACTA
BBA

www.elsevier.com/locate/bba

# Conformation and dynamic properties of a saturated hydrocarbon chain confined in a model membrane: a Brownian dynamics simulation

M.X. Fernandes [a], M.L. Huertas [b], M.A.R.B. Castanho [a,c], J. García de la Torre [b,*]

[a] *Departamento de Química e Bioquímica, Faculdade de Ciências da UL, Bl. C1-5°, Campo Grande, 1700 Lisbon, Portugal*
[b] *Departamento de Química Física, Facultad de Química, Universidad de Murcia, 30071 Murcia, Spain*
[c] *Centro de Química Física Molecular, Complexo I-IST, 1096 Lisbon, Codex, Portugal*

Received 12 May 1999; received in revised form 10 September 1999; accepted 28 September 1999

**Abstract**

A Brownian dynamics simulation of a saturated hydrocarbon chain with simple mean-field potentials, namely anchorage, orientation and enclosing, reproducing a biological membrane environment is presented. The simulation was performed for a time equivalent to 1.4 μs thanks to the simplicity of our model. The results are compared with those obtained for a hydrocarbon chain simulated in the absence of the membrane potentials but with confinement. With the appropriate choice of parameters, equilibrium properties, such as deuterium order parameter, chain length, tilt angle and geometry, and dynamic properties, such as dihedral angle transition rate, rotational and translational diffusion, recovered from our simulations, correctly reproduced, are consistent with hydrocarbon-derived molecule experimental results and simulation results obtained from other more complex studies. 

*Keywords:* Brownian dynamics simulation; Mean-field potential; Model membrane; Hydrocarbon chain

## 1. Introduction

Biological membranes are the selective envelope of living cells and the understanding of their biological functions is of crucial interest. Structural and dynamic features of biological membranes and model membrane systems have been studied both experimentally and by computer simulation. Nevertheless, the difficulties arising from the dynamic nature, finite dimensions, heterogeneous composition and the curved interface of biological membranes make it hard to fully understand the relative importance of different phospholipid motions for the global membrane system dynamics.

On our work, attention was focused on the dynamics of a simulated hydrocarbon chain embedded in a model membrane. Recent simulation studies of membrane structure and dynamics have been based on intensive computation techniques such as molecular dynamics (MD) ([1] and references therein). Due to the very detailed representation, specifying all atoms, employed by MD, only short time scale trajectories, at most a few ns, are reproduced and many significant features of membrane nature cannot be seen because they occur on a long time scale [2]. A more meaningful description of the membrane structure and dynamics comes from the use of Brownian

* Corresponding author. Fax: +34 (968) 364148; E-mail: jgt@fcu.um.es

0005-2736/00/$ – see front matter 
PII: S0005-2736(99)00188-1

dynamics (BD) simulation with atomic level detail. There are examples in the literature of development of mean-field potentials that could describe a membrane environment [3] and of application of those potentials in stochastic dynamics simulation with atomic level detail [4,5]. There were also attempts of combining MD and mean-field calculations [6,7]. De Loof et al. [6] simulated a central molecule with MD and boundary molecules with stochastic dynamics in a membrane environment. Fattal and Ben-Shaul [7] calculated conformational properties of lipid chains using a mean-field theory of chain packing statistics and MD. However, all these works have a high level of complexity and general, reliable and simple mean-field potentials suitable for stochastic computer simulations of the membrane environment are not yet available.

Seeking for simplicity, without sacrificing accuracy, in our work, only a single hydrocarbon chain is represented in terms of a detailed atom description. The interactions of this molecule with the membrane environment are represented by a set of adequate potentials and random forces. It is our aim to build up a general, and easy to implement, set of mean-field potentials that would simulate the membrane environment and reproduce the behavior of equilibrium and dynamics features of membrane components or similar molecules. The proposed model system does not submit the simulated molecules to any kind of rigid restriction like anchoring with co-ordinate fixation or rotational limitations. Confrontation of the results here obtained with NMR experimental results [8,9] and results from other simulation studies of a very different type [4,6,10] is done to ensure the validity of the system presented here. Using simple mean-field potentials and BD simulation, it is possible to reach long time scale trajectories, in the range of μs, which are needed to describe membrane dynamics correctly. A drawback of this strategy is the lack in the description of collective motions of membrane molecules or intermolecular interactions which may be important for knowledge of the membrane nature.

The results presented here validate the use of the BD technique for simulation studies of membrane systems and could be used to predict the behavior of molecules located within a membrane and the behavior of membrane components.

## 2. Materials and methods

### 2.1. Model, energetics and simulation method

The system that we consider consists of a 16 elements molecule moving in the environment of a phospholipid bilayer of a given thickness. The simulated molecule reproduces the geometry and dimensions of a saturated hydrocarbon chain with 16 carbon atoms. The methyl and methylene groups are represented by spheres joined by a frictionless connector, of which one extremity sphere tends to be anchored to the membrane boundary. The simulated system is depicted in Fig. 1 along with the potential profiles. Notice that none of the spheres of our simu-

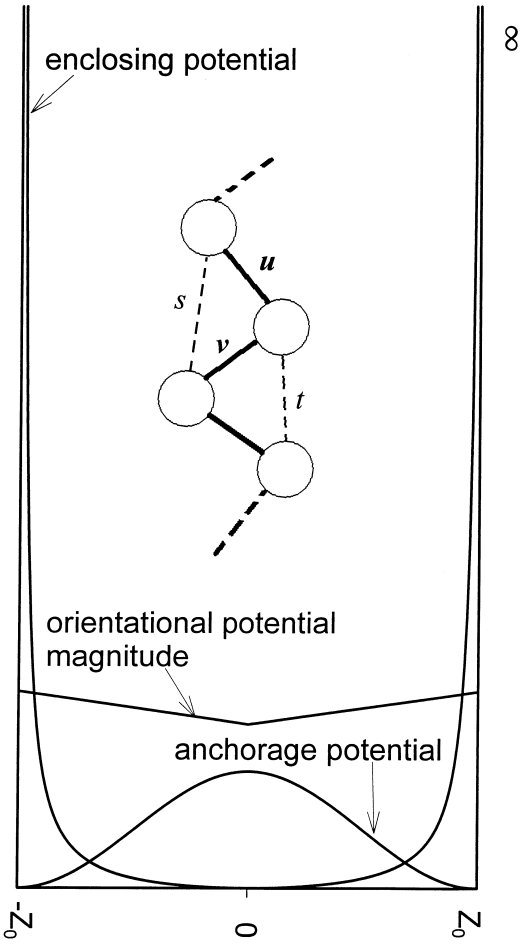


Fig. 1. A generalized chain and the profile of external potentials along the $z$ axis (bilayer normal). Bending angle $\theta$ is the angle between vectors $u$ and $v$. The torsional angle $\phi$ is the angle between plane $s$ and plane $t$.

lated chain can trespass the membrane boundaries, meaning that the chain trajectories are confined.

### 2.2. Hydrocarbon chain energetics

The total intramolecular potential considered has contributions resulting from bond length potential, bond angle potential, torsion angle potential and non-bonded pairwise interaction potential and their magnitudes [11,12] are listed in Table 1.

The bond length potential, hereafter named stretching potential, is defined by a harmonic potential that maintains the equilibrium bond length of carbon-carbon bonds and has the following expression

$$V_s = 0.5K_s(d_i - d_i^0)^2 \quad (1)$$

where $K_s$ is the spring constant, $d_i$ is the instantaneous distance between $i$ ($i=1$, ..., 15) and $i+1$ and $d_i^0$ is the distance between $i$ and $i+1$ in the equilibrium conformation.

Table 1
Parameters for the simulation of hydrocarbon chain internal energy

| Lennard-Jones potential | |
|---|---|
| Parameter | Magnitude |
| $\sigma$ | 3.92 Å |
| $\varepsilon$ | $600\times10^6$ kJ/mol |
| **Torsional potential** | |
| Parameter | Magnitude (kJ/mol) |
| $C_0$ | 8.113 |
| $C_1$ | 15.591 |
| $C_2$ | −4.476 |
| $C_3$ | −15.478 |
| $C_4$ | 8.951 |
| $C_5$ | −12.681 |
| **Bending potential** | |
| Parameter | Magnitude |
| Bond angle | 111° |
| Bending constant | 520 kJ/mol |
| **Stretching potential** | |
| Parameter | Magnitude |
| Bond length | 1.53 Å |
| Stretching constant | $1.044\times10^3$ kJ/mol/Å$^2$ |

The bond angle potential, hereafter named bending potential, has the same generic expression of that of the stretching potential, meaning that it is of the harmonic type. Its expression is

$$V_b = 0.5K_b(\theta'_i - \theta_0)^2 \quad (2)$$

where $K_b$ is the bending constant, $\theta'_i$ ($i=1$, ..., 14) is the instantaneous bending angle and $\theta_0$ is the equilibrium bending angle.

The torsional potential is given by the Ryckaert-Bellemans potential [13] expression and it is a sum that reads

$$V_\phi = \sum_{k=0}^{5} c_k\ (\cos\ \phi_i)^k \quad (3)$$

where $\phi_i$ is a dihedral angle ($i=1$, ..., 13) and $\phi=0°$ for the *trans* conformation, $\phi=120°$ and $\phi=-120°$ for $gauche_+$ and $gauche_-$, respectively.

The interaction potential for non-bonded atoms is included via a Lennard-Jones potential that has the following expression

$$V_{LJ} = 4\varepsilon\left(\left(\frac{\sigma}{r_{ij}}\right)^{12} - \left(\frac{\sigma}{r_{ij}}\right)^{6}\right) \quad (4)$$

where $r_{ij}$ is the distance between atoms $i$ and $j$, $\varepsilon$ is the depth of the potential and $\sigma$ is the distance where the Lennard-Jones potential is zero.

### 2.3. Membrane energetics

To confine the motion of simulated molecules to the interior of our model membrane, we use a hard-wall potential. This potential only acts whenever a sphere of simulated hydrocarbon chains leaves the allowed region of motion and its effect is to place the mentioned sphere once again inside the model membrane. The confinement of the chain elements to the desired region is represented by:

$$\left\{\begin{array}{l} V_{conf} = 0 \text{ if } |z| \le z_0 \\ V_{conf} = \infty \text{ if } |z| > z_0 \end{array}\right\} \quad (5)$$

To describe the membrane environment, we considered three distinct potentials. The first one takes into account the enclosure effect of the finite thickness of the model membrane [14] along the $z$ direc-

tion and has the form

$$V_{\mathrm{encl}}(z_i) = \frac{kTK_z}{(z_0^2 - z_i^2)} \quad (6)$$

where $i$ runs from two to 16, $z_i$ is the $z$ co-ordinate of the sphere $i$ of the chain, $z_0$ is the half-width of the membrane, $k$ is the Boltzmann constant, $T$ the temperature and $K_z$ the magnitude of the enclosing potential. This potential replicates in a smooth way the behavior of the hard-wall potential. We use this potential mainly to avoid triggering the hard-wall potential, since discontinuities are not very desirable. This way, and generally, the hard-wall potential only acts upon sphere 1 of the simulated chains.

The first sphere of the chain was designed to anchor to the membrane boundaries so it experiences an anchorage potential with the following expression

$$V_{\mathrm{anch}} = kTK_{\mathrm{anch}}\cos^2\left(\frac{z_1\pi}{2z_0}\right) \quad (7)$$

where $z_1$ is the $z$ co-ordinate of the first sphere of the chain and $K_{\mathrm{anch}}$ is the magnitude of the potential. This potential allows for perpendicular motion which would account for the rough membrane surface [15] and, as a possibility for the future, investigates effects like solute penetration.

To simulate the ordering effect induced by the membrane environment, a Maier-Saupe orientational potential is introduced. This potential drives the simulated chain to assume a more parallel orientation to transverse the plane of the membrane, that is to say an orientation along the $z$ axis. The field strength, $K_\theta$, of this potential is not constant throughout the membrane, reproducing the different packing of hydrocarbon tails in biological membranes determined by neutron diffraction [16], instead it changes with a linear dependence according to the distance of he membrane boundaries, meaning $K_\theta(z) = K_\theta^0 + q|z|$, being higher at the membrane boundaries and lower at the membrane interior. This linear dependence of the magnitude of the field strength, $K_\theta$, allows for the reproduction, as shown below, of the profile and magnitude of the deuterium order parameter of phospholipids [8] and other hydrocarbon-derived molecules [9] obtained by spectroscopic techniques and by computer simulation [4,10]. The potential is given by

$$V_{\mathrm{orient}} = -\frac{3}{2}kTK_\theta(z)\left(\cos^2\theta_i - 1\right) \quad (8)$$

where $K_\theta(z)$ is the field strength of the orientational potential, $\theta_i$ is the angle formed by the $z$ axis and vector that joins atoms $C_{i-1}$ and $C_{i+1}$. All the potentials and their first derivative, except the hard-wall potential, are continuous within the domain accessible to the motion of the simulated molecule.

### 2.4. Simulation method

The BD trajectories of a single molecule were simulated using a method based on the algorithm of Ermak-McCammon [17] modified by Iniesta and García de la Torre [18]. Each Brownian step is taken into account twice, in a predictor-corrector way, and the resulting positions of the elements, $r$, after a time step $\Delta t$ are obtained from the previous ones, using the following equations

$$r' = r^0 + \frac{\Delta t}{kT}D^0{\cdot}F^0 + \Delta t\,(\nabla_r D)^0 + R^0 \quad (9)$$

$$r = r^0 + \frac{\Delta t}{kT}\frac{1}{2}\left(D^0{\cdot}F^0 + D'{\cdot}F'\right) + \Delta t\,\frac{1}{2}[(\nabla_r D) + (\nabla_r D)^0] + R' \quad (10)$$

Eq. 9 is used to calculate the predictor substep whose determination is based on quantities corresponding to the initial conformation, $r^0$. In this substep, an estimate, $r'$, of the final conformation is obtained and required quantities are evaluated with that conformation. Afterwards, the corrector substep is calculated with Eq. 10, based once again on the initial conformation $r^0$, but using quantities that arise from the mean of those obtained with conformations $r^0$ and $r'$. Although one step in the procedure here described is equivalent to two steps in the Ermak-McCammon algorithm and consequently it takes about double of the CPU time of the latter, we can use longer time steps and there is an increase of efficiency [19].

The $3N$ vectors $r$ and $F$ are the co-ordinates and mechanical forces on the $N$ beads, $D$ is the $3N\times 3N$ diffusion supermatrix whose $ij$ blocks are the diffusion tensors, $D_{ij}$. $R^0$ and $R'$ are random vectors with

a covariance matrix equal to $2\Delta t D^0$ and $2\Delta t D'$, respectively. They are obtained from Gaussian-distributed vectors, with zero mean and unitary variance, $q$ and $q'$, as $R^0 = \sqrt{2\Delta t}\sigma^0 q$ or $R' = \sqrt{2\Delta t}\sigma' q'$, where $\sigma$ is a $3N \times 3N$ supermatrix obtained from the square root of $D$ [20].

When simulating dynamic properties, hydrodynamic interaction (HI) between elements of the system must be adequately taken into account. We use the modified Oseen tensor [21,22], which corrects the effects of a non-point like nature of frictional elements and eventual overlapping. The inclusion of HI is done setting, for $i \neq j$, $D_{ij} = kTT_{ij}$, where $T_{ij}$ is the modified Oseen tensor. On the other hand, when simulating equilibrium properties, HIs can be neglected because they do not have any dependence on the rate of dynamic processes. The BD without HI is less computational time consuming than BD with HI and is the most adequate to spawn the entire conformational range of simulated molecules. The exclusion of HI is done setting, for $i \neq j$, $D_{ij} = 0$ in Eq. 9. Note that in both cases, HI or no-HI, $D_{ii} = (kT/\xi_i)I$, where $I$ is a unit $3 \times 3$ matrix and $\xi_i$ the friction coefficient of the $i$th element.

In the present work, we followed the above strategy, meaning that equilibrium properties were obtained from no-HI BD trajectories and that dynamic properties and features were obtained from HI BD trajectories.

### 2.5. Parametrization of simulated system

The parameters of the potentials used in the simulated trajectories are the ones described here. The parameters for the stretching, bending, torsional and Lennard-Jones potential appear in Table 1.

A systematic search of appropriate potential magnitudes was performed and the obtained results, with each different choice of magnitudes, confronted with experimental data. Our search shows that a higher value of the orientational potential will lead to a general raise of $-S_{CD}(i)$ parameters, a higher value of the anchorage potential will produce a small raise of $-S_{CD}(i)$ parameters near the interface and a higher value of the enclosing potential has an effect of diminishing the values of $-S_{CD}(i)$ near the membranes mid plane. Of course, the effects of these potentials are interwoven and it is not possible to obtain at will the desired reproduction of experimental data. The anchorage potential constant, $K_{anch}$, used was $9.7 \times 10^{-2}$ kJ/mol, the enclosing potential constant, $K_z$, has a value of 19.38 kJ Å$^2$/mol and the orientational potential constant, $K_\theta(z)$, was set to $6.2 \times 10^{-2}$ kJ/mol, at $|z| = z_0$, and $5.2 \times 10^{-2}$ kJ/mol at $z = 0$. The potentials were set to these particular values in order to recover the characteristic deuterium order parameter profile and magnitude of a phospholipid in a membrane [8] and other derived hydrocarbon molecules [9].

The simulations were done with a 16 element chain, a membrane half-thickness, $z_0$, of 20 Å [8], at 324 K, well above the transition phase temperature (314 K) of 1,2-dipalmitoyl-3-sn-phosphatidylcholine, which is the most widely used phospholipid in model membrane studies, with a viscosity of 2.5 cP [4], with $\Delta t = 70$ fs and a total trajectory time of 1.4 μs. The trajectories thus generated were analyzed to recover equilibrium properties, as averages over each trajectory. The correlation functions were also recovered from simulated trajectories. The rotational correlation functions, $\langle P_2(t) \rangle$, where $P_2(t)$ is the second Legendre polynomial, were build up as

$$\langle P_2(t) \rangle = \langle P_2(u(t) \bullet u(0)) \rangle \quad (11)$$

$u(0)$ being an unitary vector along the extremities of the analyzed bond at one chosen initial time and $u(t)$ being the unitary vector along the same extremities after a time gap $t$. The brackets represent an average over every possible choice of the initial time. The $\langle P_2(t) \rangle$ functions were fitted to a multi-exponential with DISCRETE [23,24] and the resulting function is

$$\langle P_2(t) \rangle = a_0 + a_1 e^{(-b_1 t)} + a_2 e^{(-b_2 t)} + \ldots \quad (12)$$

The kinetics of the $\langle P_2(t) \rangle$ decay can be expressed by two characteristic relaxation times. One of them is the initial relaxation time, $\tau_{ini}$, which describes the initial rate of decay and is given by the following expression

$$\tau_{ini} = (a_1 b_1 + a_2 b_2 + \ldots)^{-1} \quad (13)$$

and the other one called mean relaxation time, $\tau_{mean}$, is expressed as

$$\tau_{mean} = \frac{(a_1/b_1 + a_2/b_2 + \ldots)}{(1 - a_0)} \quad (14)$$

and is an indication of an average rate of a normalized decay along the whole curve.

The translational dynamics can be asserted by the mean square displacement of the hydrocarbon chain mass center. For the co-ordinate $\alpha$, where $\alpha$ could be any of the three Cartesian co-ordinates, and for a time $t$, the mean square displacement is

$$\langle[\alpha(t)-\alpha(0)]^2\rangle \quad (15)$$

where the average is done over any possible choice of the initial time.

## 3. Results and discussion

In our presentation, we will show the effects, at the molecular level, of anchorage and orientation effects comparing the results of confined simulated chains submitted to these effects with results of confined simulated chains not submitted to these effects. So, when we say afterwards that a hydrocarbon chain experiences membrane potentials, we mean that all effects are present (confinement, orientation, anchorage and enclosing) and when we say that a simulated molecule does not experience membrane potentials, we mean that only the confinement effect is present.

### 3.1. Equilibrium properties

Fig. 2 shows the deuterium order parameters, $-S_{CD}(i)$, as a function of the carbon position extracted for a confined hydrocarbon chain simulated in the presence and in the absence of membrane potentials. The order parameter determined from NMR experiments gives an indication of the order in a membrane. It is associated with the orientation of the deuterium of a $CD_2$ group with respect to the transverse plane of the membrane. Since in our simulations we do not represent explicitly the hydrogen atoms, the $-S_{CD}(i)$ parameter associated to the $i$th C atom can be calculated as

$$-S_{CD}(i) = \left\langle \frac{3\cos^2\beta_i - 1}{2} \right\rangle \quad (16)$$

where $\beta_i$ is the angle between the membrane normal, meaning the $z$ axis, and the plane spanned by the two C-D vectors of the $i$th C atom, which is parallel to the vector defined from the $i-1$ to the $i+1$ C atoms.

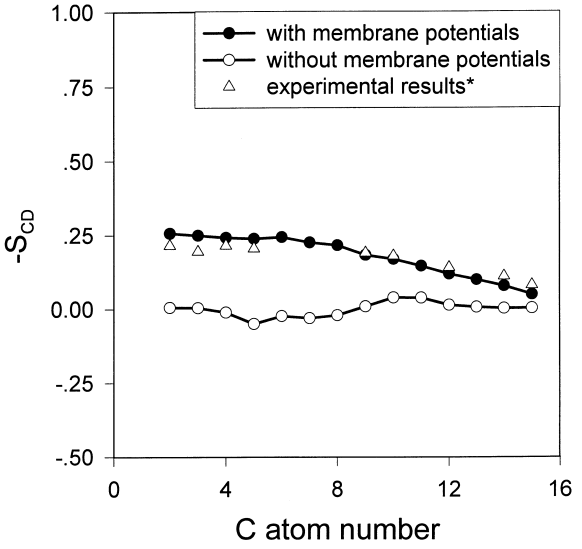


Fig. 2. Deuterium order parameter of simulated hydrocarbon chains and experimental results, obtained in similar conditions, from [8].

The $-S_{CD}(i)$ parameter can assume values between $-0.5$ (orientation parallel to the membrane interface) and one (orientation perpendicular to the membrane interface). The average presented in Eq. 16 is done over the entire trajectory.

Fig. 2 shows that the $-S_{CD}(i)$ order parameters, for the case of the chain simulated in the absence of membrane potentials, are in the vicinity of zero for all carbon positions and that they have a flat profile. This indicates that the chain has not any preference for a particular orientation. The values of the $-S_{CD}(i)$ order parameter along the hydrocarbon chain, simulated in the presence of membrane potentials, present a relatively flat profile at the beginning of the chain and then, they decrease as we move far away from the membrane interface. This result indicates that the ordering effect of the phospholipid bilayer environment is more strongly felt near the interface regions. The calculated $-S_{CD}(i)$ order parameters for the hydrocarbon chain, simulated in the presence of membrane potentials, show that it prefers an orientation that is more parallel to the transverse plane of the membrane, as it is indicated by a higher value of $-S_{CD}(i)$, compared with the orientation assumed by the chain simulated in the absence of membrane potentials. The recovered values of $-S_{CD}(i)$ are in close agreement with the ones found by other

authors [6,8,10], for related molecules, in both experimental or simulation approaches.

The percentages of the conformations for each dihedral angle of the simulated hydrocarbon chains are presented in Table 2. The dihedral angle was considered to be in one particular conformation when it assumed values of the mentioned conformation minimum $\pm 60°$, meaning until it crossed the dihedral potential barrier. It can be seen that the percentage of *trans* conformation of dihedral angles of hydrocarbon chain increases slightly when the simulation was performed in the presence of membrane potentials. This indicates that when there are external potentials applied, the simulated chain tends to be more stretched. In simulations performed in the presence of membrane potentials, there is a clear odd-even effect, i.e. the odd number dihedral angles have higher percentages of *trans* configuration than the even number dihedral angles. This effect is not so remarkable when simulation is performed in the absence of membrane potentials.

The tilt angle, here defined as the angle that the end-to-end vector makes with the $z$ axis, of the hydrocarbon chain along the simulated trajectory in the presence of membrane potentials has an average value of approximately 37°. The magnitude of this angle, along the trajectory, has values from 0 to 90°. An average tilt angle different from 0° indicates that the simulated chain on the average is not parallel to the $z$ axis.

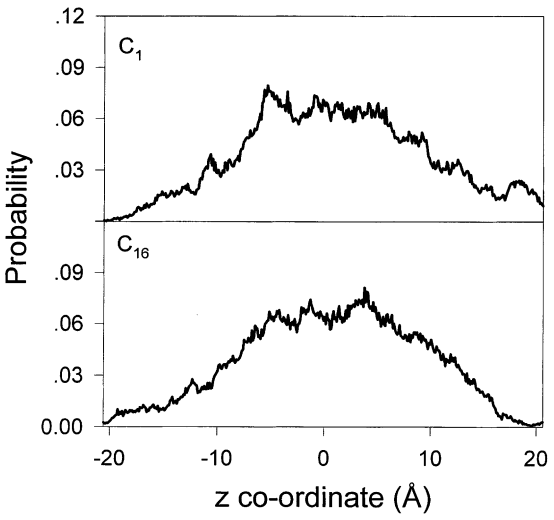


Fig. 3. Transverse position of C atoms for a simulated hydrocarbon chain without membrane potentials.

The tilt angle of the hydrocarbon chain obtains an average value of 87°, along the simulated trajectory in the absence of membrane potentials. The magnitude of this angle, along this trajectory, obtains values from 0 to 180°. An average tilt angle close to 90° implies that the hydrocarbon chain covers the entire domain of possible conformations since this chain is

Table 2
Dihedral angles population for a hydrocarbon chain simulated in the presence of membrane potentials and in the absence of membrane potentials

| Dihedral angle | With membrane potentials | | Without membrane potentials | |
|---|---|---|---|---|
| | % of *trans* state | % of *gauche* state | % of *trans* state | % of *gauche* state |
| 1 | 64 | 37 | 61 | 39 |
| 2 | 71 | 29 | 66 | 34 |
| 3 | 63 | 37 | 66 | 34 |
| 4 | 74 | 26 | 59 | 41 |
| 5 | 55 | 45 | 57 | 43 |
| 6 | 75 | 25 | 63 | 37 |
| 7 | 58 | 42 | 62 | 38 |
| 8 | 69 | 31 | 62 | 38 |
| 9 | 64 | 36 | 69 | 31 |
| 10 | 61 | 39 | 62 | 38 |
| 11 | 67 | 33 | 63 | 37 |
| 12 | 66 | 33 | 69 | 30 |
| 13 | 61 | 39 | 56 | 44 |

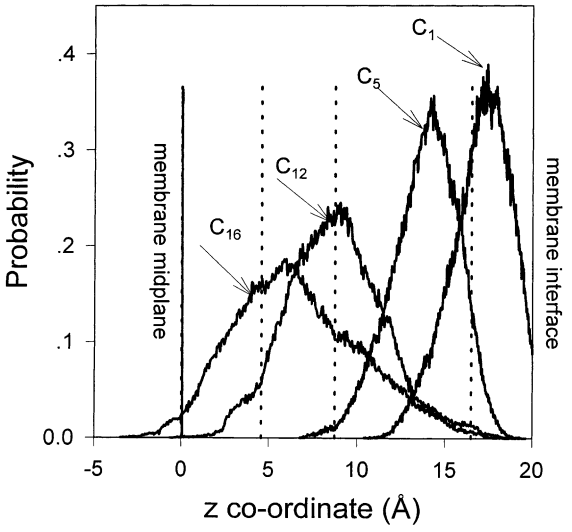


Fig. 4. Transverse position of C atoms for a simulated hydrocarbon chain with membrane potentials. The dashed vertical lines represent the positions of $C_5$, $C_{12}$ and $C_{16}$ in a full extended hydrocarbon chain with $C_1$ placed at the membrane interface.

not submitted to any orientational potential and can move freely within the membrane.

The hydrocarbon chain end-to-end length has an average value of 13.70 Å along the simulated trajectory in the presence of membrane potentials. This value is in very good agreement with the value of 13.15 Å obtained experimentally [8] and can be compared with the value of 16.08 Å for the full extended hydrocarbon chain. A shorter chain length is due to bends and tilts. The average hydrocarbon chain end-to-end length obtained from simulation in the absence of membrane potentials is 12.55 Å, smaller than the average length obtained for the hydrocarbon chain simulated in the presence of membrane potentials, but similar to the average end-to-end length, 12.29 Å, extracted from the simulation of a not confined free hydrocarbon chain. This similarity of results obtained for the confined hydrocarbon chain and the free hydrocarbon chain is due to the small effect of confinement, since the hydrocarbon chain average length is small compared to the membrane thickness.

When the hydrocarbon chain was simulated in the absence of membrane potentials, we obtained a profile for the transverse position of atoms $C_1$ and $C_{16}$, which is shown in Fig. 3. We can see that any of the considered atoms share the same distribution profile and that on average, they tend to be located in the middle of the membrane.

Fig. 4 shows the $z$ co-ordinate, that is to say the transverse position, of atoms $C_1$, $C_5$, $C_{12}$ and $C_{16}$, extracted from the simulated trajectory of a hydrocarbon in the presence of membrane potentials. It is perceptible that the $C_{16}$ tends to be closer to the membrane interface, the $C_{12}$ does not have a noteworthy change and $C_1$ and $C_5$ tend to be further away from the membrane interface, when the positions are compared with the ones of the full extended chain with $C_1$ positioned at the membrane interface, that are drawn as dashed vertical lines.

### 3.2. Dynamic properties

A study of dihedral angle conformation transition rates, *trans-gauche, gauche-trans* and *gauche-gauche*, was performed and the extracted values for all dihedral angles in simulation performed with membrane potentials appear in Fig. 5. The same study was done for the hydrocarbon chains simulated in the absence of membrane potentials and similar results were obtained. We considered a transition when the dihedral angle value overcame the potential barrier and crossed the corresponding dihedral potential local minimum. This way, we do not count temporary leaps as true transitions. Assuming that the transitions are independent, the transition rate is obtained

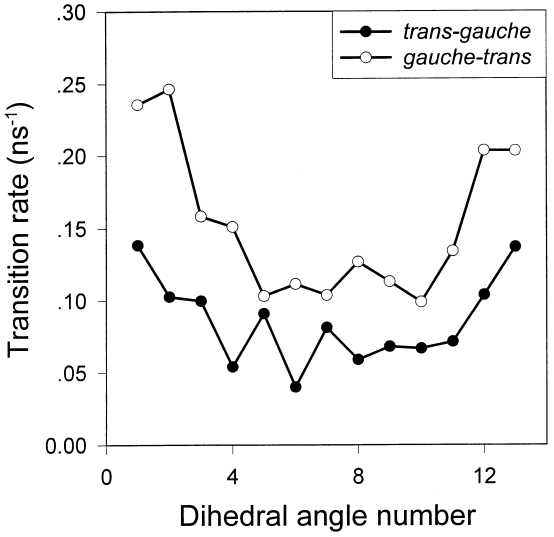


Fig. 5. Dihedral angle transition rate for a hydrocarbon chain simulated with membrane potentials.

by dividing the number of transitions from a particular conformation by the total time spent in that conformation. The transition rates between the different dihedral angle conformations along the simulated trajectories show remarkable differences if we compare extremity dihedral angles with inner dihedral angles. The extremity dihedral angles present higher transition rates than inner angles and as in the case of the *trans/gauche* population percentage, there is an odd-even effect, which cannot be assigned to statistical fluctuations. This effect was also reported before in other kind of simulation [9]. The *gauche-trans* rate is higher than the *trans-gauche* rate, which is logical since the potential barrier in the first situation is lower than in the second. The *gauche-gauche* rate is for all dihedral angles in the vicinity of zero. The counted number of these transitions was generally zero or at most one.

Results for the rotational correlation analysis of the C-C bonds are shown in Table 3 and the corresponding $\langle P_2(t)\rangle$ correlation functions in Fig. 6. Table 3 shows that the $\tau_{ini}$ and $\tau_{mean}$ parameters show a trend to increase from the extremities to the middle of the simulated hydrocarbon chains in the presence and in the absence of membrane potentials, meaning that extremities have a higher rotational freedom.

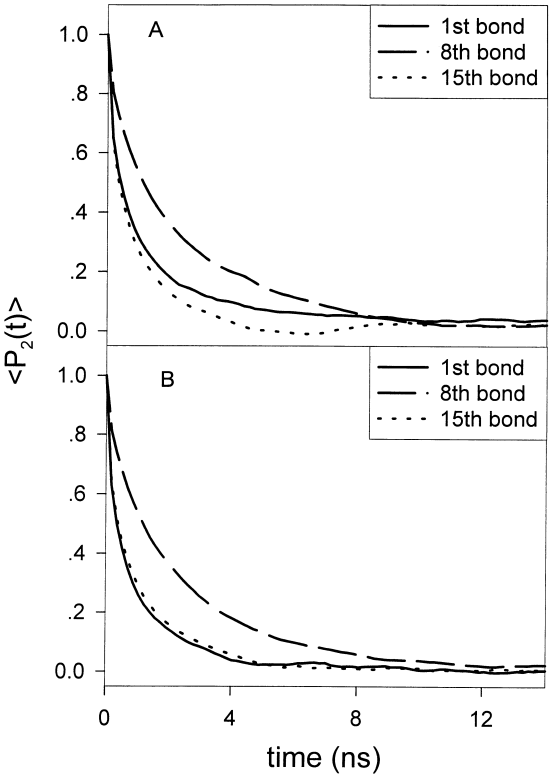


Fig. 6. Rotational correlation analysis of C-C bonds: (A) Simulations with membrane potentials, (B) simulations without membrane potentials.

Table 3
Rotational correlation analysis results of C-C bonds for hydrocarbon chains simulated in the presence and in the absence of membrane potentials

| Bond | With membrane potentials | | Without membrane potentials | |
|---|---|---|---|---|
| | $\tau_{ini}$ | $\tau_{mean}$ | $\tau_{ini}$ | $\tau_{mean}$ |
| 1 | 0.518 | 1.370 | 0.480 | 1.231 |
| 2 | 0.574 | 1.788 | 0.568 | 4.908 |
| 3 | 0.902 | 2.356 | 0.616 | 2.170 |
| 4 | 0.716 | 2.631 | 1.666 | 3.464 |
| 5 | 1.135 | 2.879 | 1.663 | 2.933 |
| 6 | 0.806 | 3.886 | 2.060 | 3.651 |
| 7 | 1.300 | 3.241 | 1.166 | 2.861 |
| 8 | 1.475 | 3.317 | 1.214 | 2.971 |
| 9 | 1.374 | 3.488 | 1.229 | 2.946 |
| 10 | 1.073 | 2.672 | 1.282 | 3.066 |
| 11 | 0.709 | 2.649 | 1.294 | 2.904 |
| 12 | 1.918 | 3.788 | 1.119 | 2.630 |
| 13 | 0.708 | 1.849 | 0.921 | 2.207 |
| 14 | 0.717 | 1.669 | 0.576 | 1.527 |
| 15 | 0.401 | 1.102 | 0.486 | 1.378 |

This tendency is very sharp when we consider the simulated chain in the presence of membrane potentials. The tendency is not so sharp for the situation of the chain simulated in the absence of membrane potentials. We cannot reach definite conclusions because the associated errors to these values are around 10%. The extremities of the hydrocarbon chain are not equivalent, what concerns rotational properties, for the situation where the chain experiences the membrane potentials, the $C_{16}$ extremity having more rotational freedom, meaning faster relaxation, than the $C_1$ extremity. When simulated in the absence of membrane potentials, the $C_1$ and $C_{16}$ extremities of the hydrocarbon chain have an equivalent degree of rotational freedom.

The results of correlation analysis for the translation along the $x$ axis and along the $y$ axis are equivalent for the hydrocarbon chains simulated in the presence and in the absence of membrane potentials. Along these directions, the hydrocarbon chain behaves like a free moving particle, meaning that the

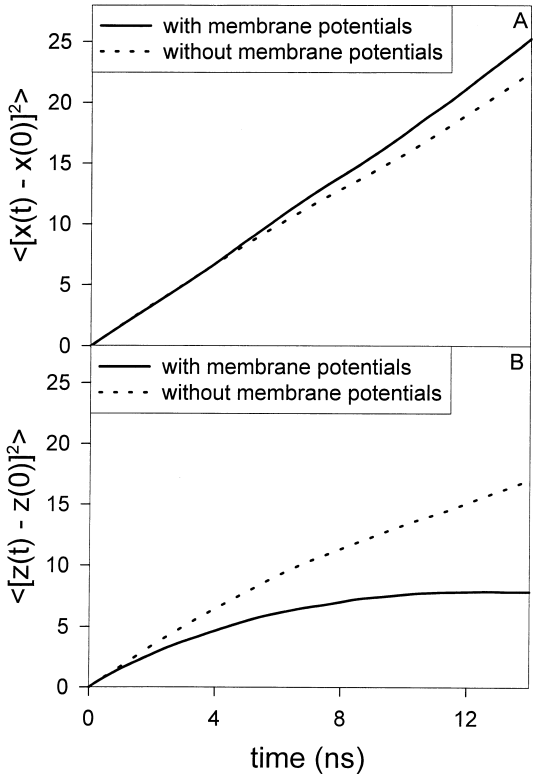


Fig. 7. Translational correlation analysis of hydrocarbon mass center: (A) results for $x$ co-ordinate, (B) results for $z$ co-ordinate.

mean square displacement is invariant with time which is presented in Fig. 7A. We extracted lateral diffusion coefficients from the mean squared displacement of the mass center of the hydrocarbon chain, using

$$\lim_{t\to\infty}\langle\alpha^2(t)\rangle = 4Dt \tag{17}$$

with

$$\alpha^2(t) = [x(t)-x(0)]^2 + [y(t)-y(0)]^2 \tag{18}$$

and obtained values around $1.6\times10^{-7}$ cm$^2$/s for both cases. This value agrees well with values obtained experimentally [25,26].

The correlation analysis of translation along the $z$ axis does not produce equivalent results for the simulated hydrocarbon chains in the presence and in the absence of membrane potentials. The theoretical treatment of the diffusity which deals with the question of anisotropic translation of a particle was presented elsewhere [14]. Since the movement along this direction is restricted, due to the finite thickness of the simulated membrane, the $z$ mean square displacement reaches a plateau. This plateau is reached earlier, and it is lower, for the hydrocarbon chain simulated in the presence of membrane potentials than for the chain simulated in the absence of membrane potentials as it is shown in Fig. 7B. This last result happens due to the presence of the anchorage potential which restricts furthermore the motion along the $z$ direction.

## 4. Conclusions

We propose a simple mean-field approach to simulate, by BD, a biological membrane environment and the properties of a hydrocarbon chain confined therein. The simplicity of our proposal allows for a feasible, long time range and easy to implement simulation from which we recover equilibrium properties such as geometry, atom distribution, chain length, tilt angle and deuterium order parameter of the simulated chain. The recovered values agree quite well with experimental and simulation results obtained by other techniques.

Dynamic properties such as transition rates, correlation functions for rotation, $\langle P_2(t)\rangle$, and correlation functions for translation, $\langle[\alpha(t)-\alpha(0)]^2\rangle$, can also be obtained from our simulations. The recovered values for the lateral diffusion coefficient are in close agreement with those obtained experimentally.

The simulation of hydrocarbon chains with and without membrane potentials did not produce remarkable effects on the internal dynamics of the hydrocarbon chains whose results in both situations are quite similar. The presence or absence of membrane potentials only affects in a noteworthy way the localization, orientation and other whole chain properties like diffusion or geometry.

In summary, we can say that the proposed model can be used to predict the equilibrium properties, dynamic properties and behavior of a hydrocarbon chain or derived molecules confined in a biological membrane. This way could be a helpful tool to bring light on some subjects such as localization, orientation and dynamics of membrane components or derived probes which are crucial for correct knowledge of biological membranes structure and dynamics.

## Acknowledgements

We thank Fundação para a Ciência e Tecnologia (Portugal) for Grant PRAXIS XXI BD/9393/96 to M.X.F., Dirección General de Enseñaza Superior (Spain) for Grant PB 96-1106 and for a predoctoral fellowship to M.L.H., Grant CI1*CT940124 from the Comission of the European Community and Grant 01758/CV/98 from Fundación Séneca.

## References

[1] D.P. Tieleman, S.J. Marrink, H.J.C. Berendsen, A computer perspective of membranes: molecular dynamics studies of lipid bilayer systems, Biochim. Biophys. Acta 1331 (1997) 235–270.
[2] E. Rommel, F. Noack, P. Meier, G. Kothe, Proton spin relaxation dispersion studies of phospholipid membranes, J. Phys. Chem. 92 (1988) 2981–2987.
[3] S. Marcelja, Chain ordering in liquid crystals II. Structure of bilayer membranes, Biochim. Biophys. Acta 367 (1974) 165–176.
[4] R.W. Pastor, R.M. Venable, M. Karplus, Brownian dynamics of a lipid chain in a membrane bilayer, J. Chem. Phys. 89 (1988) 1112–1127.
[5] R.W. Pastor, R.M. Venable, M. Karplus, A. Szabo, A simulation based model of NMR $T_1$ relaxation lipid bilayer vesicles, J. Chem. Phys. 89 (1988) 1128–1140.
[6] H. DeLoof, S.C. Harvey, J.P. Segrest, R.W. Pastor, Mean field stochastic molecular dynamics simulation of a phospholipid in a membrane, Biochemistry 30 (1991) 2099–2113.
[7] D.R. Fattal, A. Ben-Shaul, Mean-field calculations of chain packing and conformational statistics in lipid bilayers: comparison with experiments and molecular dynamics, Biophys. J. 67 (1994) 983–995.
[8] A. Seelig, J. Seelig, The dynamic structure of fatty acyl chains in a phospholipid bilayer measured by deuterium magnetic resonance, Biochemistry 13 (1974) 4839–4845.
[9] J. Seelig, W. Niederberger, Two pictures of a lipid bilayer. A comparison between deuterium label and spin-label experiments, Biochemistry 13 (1974) 1585–1588.
[10] E. Egberts, H.J.C. Berendsen, Molecular dynamics simulation of a smectic liquid crystal with atomic detail, J. Chem. Phys. 89 (1988) 3718–3732.
[11] G. Lamm, A. Szabo, Langevin modes of macromolecules, J. Chem. Phys. 85 (1986) 7334–7348.
[12] A. Rey, A. Kolinski, J. Skolnick, Y.K. Levine, Effect of double bonds on the dynamics of hydrocarbon chains, J. Chem. Phys. 97 (1992) 1240–1249.
[13] J.P. Ryckaert, A. Bellemans, Molecular dynamics of liquid n-butane near its boiling point, Chem. Phys. Lett. 30 (1975) 123–125.
[14] M.L. Huertas, V. Cruz, J.J. López Cascales, A.U. Acuña, J. García de la Torre, Distribution and diffusivity of a hydrophobic probe molecule in the interior of a membrane: theory and simulation, Biophys. J. 71 (1996) 1428–1439.
[15] J.F. Nagle, R. Zhang, S. Tristarn-Nagle, W.J. Sun, H.I. Petrache, R.M. Suter, X-ray structure determination of fully hydrated L-$\alpha$ phase dipalmitoylphosphatidylcholine bilayers, Biophys. J. 70 (1996) 1419–1431.
[16] M.C. Wiener, S.H. White, Structure of a fluid dioleylphosphatidylcholine bilayer determined by joint refinement of X-ray and neutron diffraction data III. Complete structure, Biophys. J. 61 (1992) 434–447.
[17] D.L. Ermak, J.A. McCammon, Brownian dynamics with hydrodynamic interactions, J. Chem. Phys. 69 (1978) 1352–1357.
[18] A. Iniesta, J. García de la Torre, A second-order algorithm for the simulation of the Brownian dynamics of macromolecular models, J. Chem. Phys. 92 (1990) 2015–2019.
[19] G. Chirico, J. Langowski, Calculating the hydrodynamics properties of DNA through a second-order Brownian dynamics algorithm, Macromolecules 25 (1992) 769–775.
[20] S. Allison, J. McCammon, Transport properties of rigid and flexible macromolecules by Brownian dynamics simulation, Biopolymers 23 (1984) 167–187.
[21] J. Rotne, S. Prager, Variational treatment of hydrodynamic interaction in polymers, J. Chem. Phys. 50 (1969) 4831–4837.
[22] H. Yamakawa, Transport properties of polymer chains in dilute solution: Hydrodynamic interaction, J. Chem. Phys. 53 (1970) 436–443.
[23] S. Provencher, An eigenfunction expansion method for the analysis of exponential decay curves, J. Chem. Phys. 64 (1976) 2272.
[24] S. Provencher, A Fourier method for the analysis of exponential decay curves, Biophys. J. 16 (1976) 151–170.
[25] M.E. Johnson, D.A. Berk, D. Blankschtein, D.E. Golan, R.K. Jain, R.S. Langer, Lateral diffusion of small compounds in human stratum corneum and model lipid bilayer systems, Biophys. J. 71 (1996) 2656–2668.
[26] G.J. Schutz, H. Schindler, T. Schmidt, Single-molecule microscopy on model membranes reveals anomalous diffusion, Biophys. J. 73 (1997) 1073–1080.